ChemComm

COMMUNICATION

View Article Online
View Journal | View Issue

Cite this: *Chem. Commun.*, 2026, **62**, 8417

Received 13th February 2026,
Accepted 25th March 2026

DOI: 10.1039/d6cc00836d

rsc.li/chemcomm

Squaratides: a tunable platform for anion binding in peptide-inspired macrocycles

Farhad Ali. Mohammed, [ab] Hua Tong,[a] Chris S. Hawes, [c] Shayon Bhattacharya, [bd] Damien Thompson, [be] Katrina A. Jolliffe [f] and Robert B. P. Elmes *[abg]

We report a new class of sequence-defined peptidomimetic macrocycles, termed squaratides, that incorporate squaramide units into a tunable peptide backbone. These modular receptors can bind acetate and chloride ions where sidechain functionality can control affinity and stoichiometry.

Designed artificial receptors that mimic natural systems in their ability to bind selectively to a target ion[1–4] provide molecular connectivity for supramolecular assemblies for diverse applications ranging from sustainable electronics to molecular medicine.[5,6] Nature's modular protein construction enables exquisite anion recognition through complementary hydrogen-bonding interactions (*e.g.*, the hydroxymethyl and guanidino sidechains of Ser and Arg, respectively) reinforced by backbone amides, creating preorganised cavities that bind anions with remarkable affinity and selectivity.[7–9]

Several groups have reported sequence-defined scaffolds that incorporate abiotic elements to enhance molecular recognition. For example, Jolliffe and co-workers designed cyclic and linear peptide based receptors for sulphate recognition[7,8,10,11] while Kubik *et al.* incorporated 3-aminobenzoic acids and 6-aminopicolinic acids into peptidomimetic macrocycles for cation and anion recognition.[12–14] Knipe *et al.* synthesised α-helical and β-strand peptidomimetics based on pyrimidines, while Meisel and Hamilton reported cavitand-like molecular containers derived from 2,4-dialkoxy-*meta*-aminomethylbenzoic acid (MAMBA) monomers.[15] Alfonso *et al.* synthesised a family of tris-pyridine-decorated cyclic peptides that self-assemble to carry out chloride recognition and transport.[16,17] The common feature among these examples is the judicious incorporation of abiotic building blocks into peptide scaffolds to expand the chemical design space.[7,12]

However, few sequence-defined scaffolds integrate additional hydrogen-bonding capacity directly into the peptide backbone, even though doing so could improve anion affinity and selectivity.[18–20] Here, we report a first in class family of sequence-defined macrocyclic peptidomimetics (Fig. 1(i)), termed "*squaratides*". These modular receptors embed squaramide units directly within the peptidomimetic backbone while allowing programmable sidechain functionality. Our design rationale was to couple the strong, directional hydrogen-bond donating properties of squaramides with the structural preorganisation imposed by macrocyclisation, while retaining amino acid sidechains to tune the platforms chemical properties systematically. We present a general synthetic route to create squaratides and comprehensively characterise their structures and anion-binding behaviour using NMR, IR and CD spectroscopy, X-ray crystallography, and DFT calculations. We demonstrate that macrocyclisation enhances preorganisation and thus binding selectivity toward biologically relevant anions such as acetate and chloride, and that amino acid sidechain identity profoundly influences both binding affinity and stoichiometry. Together, these findings establish squaratides as a versatile new platform for programmable anion recognition.

The synthesis of cyclic squaratides is outlined in Fig. 1(ii) where a modular, convergent strategy was employed in which diethyl squarate was sequentially functionalised with ethylenediamine and amino acid building blocks, followed by intramolecular macrocyclisation to afford a series of the sequence-defined peptidomimetic receptors. Briefly, reaction of diethyl squarate with *N*-Boc-ethylenediamine furnished the monosubstituted intermediate **A**, which was subsequently reacted with the desired amino acid before TFA initiated Boc deprotection yielded monomer **B**. Dimerisation in the presence of benzotriazol-1-yloxytripyrrolidinophosphonium

[a] *Department of Chemistry, Maynooth University, National University of Ireland, Maynooth, Co, Kildare, Ireland. E-mail: robert.elmes@mu.ie*
[b] *SSPC – the Research Ireland Centre for Pharmaceuticals, University of Limerick, V94 T9PX, Limerick, Ireland*
[c] *School of Chemical and Physical Sciences, Keele University, Keele, ST5 5BG, UK*
[d] *Department of Biological Sciences, Bernal Institute, University of Limerick, V94 T9PX, Limerick, Ireland*
[e] *Department of Physics, Bernal Institute, University of Limerick, V94 T9PX, Limerick, Ireland*
[f] *ARC Centre of Excellence for Innovations in Peptide and Protein Science, School of Chemistry, University of Sydney, 2006, NSW, Australia*
[g] *Kathleen Lonsdale Institute for Human Health Research, Maynooth University, National University of Ireland, Co. Kildare, W23 F2H6, Maynooth, Ireland*

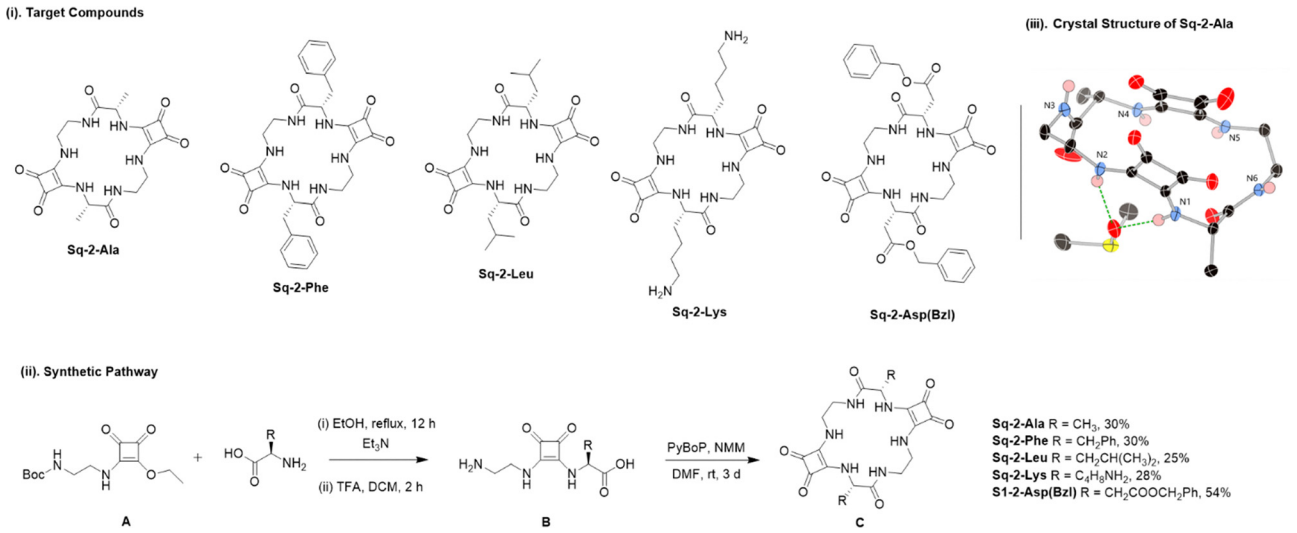

Fig. 1 (i). Chemical structures of target cyclic squaratides. (ii) General synthetic strategy towards cyclic squaratides. (iii) Crystal structure of **Sq-2-Ala**.

hexafluorophosphate (PyBOP), afforded a series of cyclic squaratides **C** in yields from 25–54%.

Single crystals of **Sq-2-Ala** grown from dilute DMSO-d_6 confirmed the cyclic structure by X-ray crystallography. The structure was solved in the chiral monoclinic space group $P2_1$ as a bis-DMSO solvate. As shown in Fig. 1(iii), the squaramide units adopt a syn conformation with both N–H donor pairs (N1, N2 and N4, N5) oriented in the same direction. Macrocycle puckering offsets the cyclobutene rings such that each functions independently as a bis-bidentate, rather than tetradentate, hydrogen-bond donor toward a single oxygen acceptor. The alanine methyl groups project towards the macrocycle periphery which suggests that side chain functionalisation may not sterically hinder anion binding.

To provide a molecular-level framework for the anion-binding behaviour of the cyclic squaratide platform, DFT calculations were performed on host–guest complexes of **Sq-2-Ala** with Cl^-, Br^-, I^-, and NO_3^-. Geometries were optimised in the gas phase from the experimental XRD structure, followed by counterpoise (CP) correction for basis set superposition error (BSSE) (see SI). The resulting BSSE-corrected binding energies (ΔE_{bind}) enable comparison across the anion series. The calculated energies follow the order $Cl^- > Br^- > I^- \gg NO_3^-$, with ΔE_{bind} values of −3.30, −3.08, −2.44, and −0.53 eV, respectively (Fig. 2e). It should be noted that these binding energies are calculated for gas-phase complexes and therefore represent an upper theoretical limit to host–guest interactions in the absence of solvent. In solution, competition with solvent molecules, particularly strongly coordinating solvents such as DMSO, is expected to weaken the effective binding interactions observed experimentally. This affinity trend reflects progressively weaker binding with increasing halide size and decreasing basicity, while NO_3^- binds much more weakly due to poor geometric complementarity with the preorganised hydrogen-bond donor array of **Sq-2-Ala**. Analysis of the optimised geometries provides further insight into this selectivity (Fig. 2a–d). In the halide complexes, Cl^- and Br^- form multiple short N–H···X^- contacts, several <2.5 Å (bold in Fig. 2), consistent with strong directional hydrogen bonding. In contrast, I^- shows fewer short contacts and more elongated N–H···I^- interactions, consistent with its weaker binding energy. For

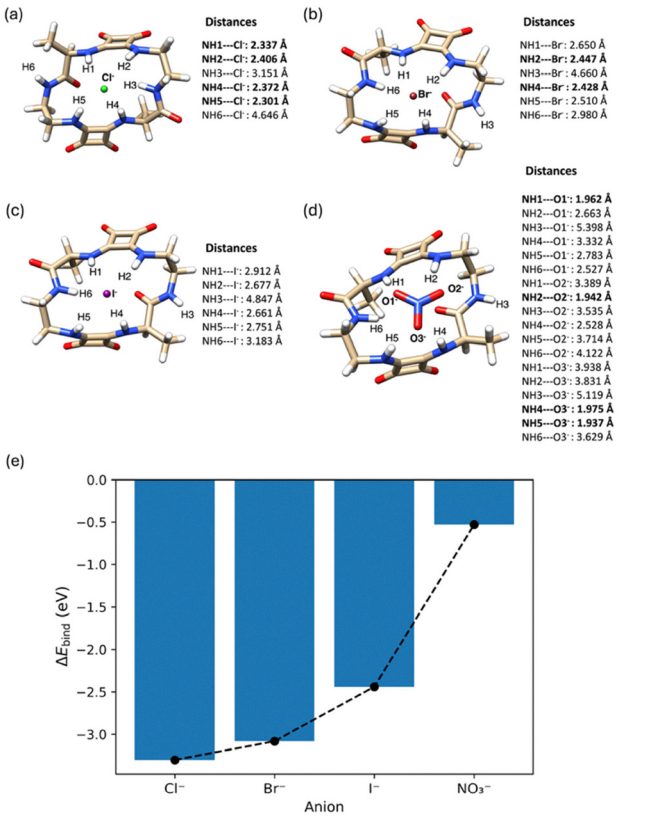

Fig. 2 DFT analysis of anion binding to **Sq-2-Ala**. (a)–(d) Optimised gas-phase geometries of **Sq-2-Ala** in complex with Cl^-, Br^-, I^-, and NO_3^-, respectively, with key N–H···anion distances annotated. Hydrogen-bond contacts shorter than 2.5 Å are highlighted in bold. (e) BSSE-corrected binding energies (ΔE_{bind}) for **Sq-2-Ala** with the anion series, showing a clear preference for smaller, more basic halides and poor affinity for nitrate.

NO_3^-, the anion remains offset from the macrocyclic cavity centre, forming only one or two short N–H···O contacts while the remaining donors remain uncoordinated, resulting in much weaker stabilisation. Side-view representations (Fig. S100, SI) show that halides sit close to the squaramide core of **Sq-2-Ala**, whereas NO_3^- resides significantly above the hydrogen-bond donor plane. This separation limits cooperative binding and accounts for the predicted energetic penalty for NO_3^- relative to the halides. Although absolute binding energies are likely overestimated in the gas phase, the BSSE-corrected calculations reproduce the experimentally relevant relative anion preference of **Sq-2-Ala** for monovalent anions reported below. These calculations provide a structural and energetic framework for interpreting the NMR titration data, supporting a model in which strong directional squaramide hydrogen bonding underpins chloride recognition, whereas larger or geometrically mismatched anions interact only weakly and are not selectively bound. Additional computational studies of competing solvent binding and alternative guest species, including DMSO, fluoride (with possible deprotonation pathways), and hydroxide, are underway and will be reported in future work. Guided by the structural analysis and modelling, the binding behaviour of **Sq-2-Ala** was investigated in DMSO-d_6 by ^{1}H NMR spectroscopy. Initial screening against eight tetrabutylammonium (TBA) salts of halides and oxoanions (F^-, Cl^-, Br^-, I^-, SO_4^{2-}, AcO^-, $H_2PO_4^-$, NO_3^-) revealed varying responses as a function of anion concentration. Deprotonation occurred upon addition of F^-, evidenced by a downfield triplet at *ca.* 16 ppm characteristic of hydrogen difluoride (HF_2^-) formation and consistent with fluoride-induced deprotonation of the squaramide NH groups.[21] In contrast, minimal shifts were observed for I^-, Br^- and NO_3^-, indicating negligible binding consistent with previous reports of weak iodide and nitrate binding.[22,23] Although gas-phase DFT calculations predict moderate Br^- binding relative to Cl^-, the negligible experimental binding likely reflects solvent competition and reduced hydrogen-bond directionality in solution, highlighting the tendency of gas-phase calculations to overestimate absolute binding energies.

The weak responses observed for the larger halides and NO_3^- are consistent with the reduced directional hydrogen bonding and geometric mismatch identified in the DFT calculations. Minor perturbations were observed in the presence of SO_4^{2-}, contrasting with the high sulfate affinity reported for other cyclic squaramides[24] and suggesting steric or geometric constraints within the squaratide cavity that hinder optimal sulfate coordination. Upon incremental addition of AcO^-, the amide NH signal shifted upfield then downfield, while the squaramide NH signals shifted downfield ($\Delta_{ppm} \approx 1.5$ for both). This behaviour suggests a concentration-dependent process in which weak, transient interactions at low AcO^- concentrations—likely involving conformational rearrangement and steric fit of the small methyl group (vdW radius ~0.2 nm, similar to the halide series, Fig. 2e)—are followed by direct hydrogen bonding at higher anion concentrations (Fig. 3a). Upon Cl^- addition, the NH signals exhibited similar but smaller shifts than for AcO^- ($\Delta_{ppm} \approx 0.6$ and 0.9).

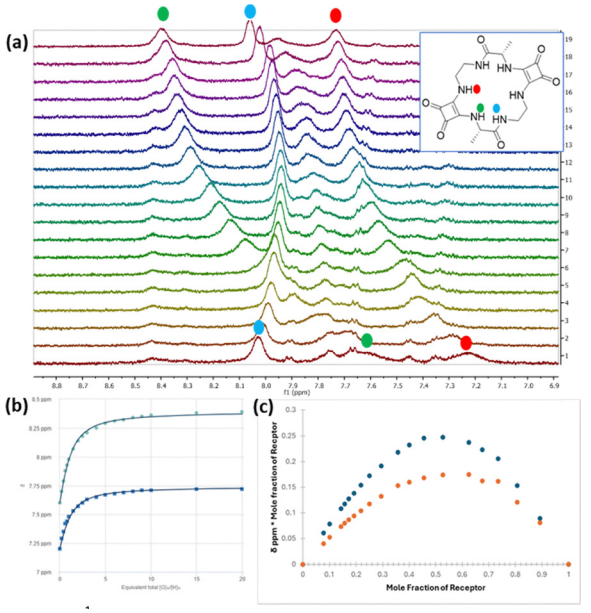

Fig. 3 (a) ^{1}H NMR Titration of **Sq-2-Ala** in DMSO-d_6 with TBACl (b) Fitted data of the chemical shift change of the NHs of **Sq-2-Ala** against molar equivalents of TBACl. (c) Jobs plot analysis of squaramide NHs of **Sq-2-Ala**.

Association constants for Cl^- and AcO^- were determined by fitting the squaramide NH chemical shift changes as a function of anion concentration using BindFit.[25]

Sq-2-Ala exhibited 1 : 1 binding stoichiometry toward both anions, with higher affinity for Cl^- (K_a = 692 M^{-1}) than AcO^- (K_a = 227 M^{-1}). This chloride affinity is comparable to highly electron-deficient diaryl squaramides and suggests that macrocyclic preorganisation, rather than increased intrinsic hydrogen-bond donor strength, underpins the observed binding enhancement.[26] The 1 : 1 binding model was supported by Job-plot analyses showing maxima at 0.5 mole fraction (Fig. 3b and c) and by independent fitting using Musketeer,[27] which yielded comparable association constants. Variation of side-chain functionality significantly modulates binding affinity and stoichiometry across the receptor series. For example, **Sq-2-Phe** displayed a 2 : 1 (host:guest) binding mode ($K_{11} = 8.3 \times 10^3$ M^{-1}, $K_{21} = 3 \times 10^3$ M^{-1}), supported by Job-plot analysis. However, deviations in the fitting residuals suggest coexisting equilibria or multiple binding geometries, and the extracted constants should be interpreted with caution. This behaviour likely arises from hydrophobic effects and π–π interactions that complicate anion binding. Nevertheless, all receptors show significant Cl^- and AcO^- binding under these conditions, underscoring the role of side-chain polarity and steric profile in tuning anion recognition (Table 1).

To further investigate the complex binding behaviour observed during anion titrations, a concentration-dependent ^{1}H NMR study of **Sq-2-Phe** was conducted over 0.25–20 mM (Fig. S95, SI). The ^{1}H NMR spectra of these squaratides were previously noted to be poorly resolved in DMSO-d_6 despite LCMS evidence of compound purity, suggesting that conformational heterogeneity and/or molecular self-assembly may

Table 1 Summary of Cl^- and AcO^- binding of cyclic squaratides. Association constants derived from Bindfit

Receptor	Cl^- (M^{-1})	Jobs plot	AcO^- (M^{-1})	Jobs plot
Sq-2-Ala	K_a = 692 (±6)	1 : 1	K_a = 227 (±3) M^{-1}	1 : 1
Sq-2-Phe	K_a = 366 (±4)	1 : 1	K_{11} = 8.3 × 10^3 (±69) K_{21} = 3 × 10^3 (±68)	2 : 1
Sq-2-Leu	K_a = 558 (±2)	1 : 1	$K_{21} > 10^4$	2 : 1
Sq-2-Lys	K_{11} = 1.8 × 10^3 (±3) K_{21} = 703 (±9)	2 : 1	K_a = 333 (±12)	1 : 1
Sq-2-Asp(Bzl)	$K_{21} > 10^4$	2 : 1	$K_{11} > 10^4$	2 : 1

contribute to the observed behaviour. For **Sq-2-Phe**, broad concentration-dependent changes were observed, particularly in the aromatic and squaramide NH regions. Increasing concentration led to (i) chemical shift changes, (ii) significant signal broadening, particularly for NH resonances, and (iii) the appearance of new signals. These features are characteristic of supramolecular self-association, consistent with intermolecular squaramide hydrogen bonding and π–π stacking of phenylalanine side chains. In contrast, while **Sq-2-Ala** also displayed poorly resolved ^{1}H NMR spectra, chemical shifts were largely concentration-invariant across the same range (Fig. S96, SI), suggesting that this receptor does not engage in aggregation to the same extent but conformational isomerism (including *cis–trans* amide isomerism as well as *anti*/*anti*- and *anti*/*syn*- conformations of bis-secondary squaramides) is likely to be a contributor. This observation further highlights the role of amino-acid identity in governing supramolecular behaviour.

To assess the influence of macrocyclisation, the acyclic analogue **ASq-2-Phe** was synthesised (Scheme S2, SI). Although its ^{1}H NMR spectra indicated conformational heterogeneity typical of acyclic peptidomimetics and foldamers,[28,29] concentration-dependent studies showed minimal aggregation, with resonances remaining relatively sharp across 0.25–20 mM (Fig. S97, SI). This contrast indicates that cyclisation in **Sq-2-Phe** enforces preorganisation and spatial proximity between squaramide and aromatic units, promoting ordered aggregation, whereas the greater flexibility of **ASq-2-Phe** suppresses this behaviour. ^{1}H NMR titration of **ASq-2-Phe** with TBA AcO^- revealed complex, multi-site binding behaviour. Larger downfield shifts at the methyl ester terminus relative to the Boc-protected end indicate uneven binding along the flexible scaffold. Up to one equivalent of AcO^-, binding occurs mainly at the squaramide units, with backbone amide NHs engaging only at higher anion loadings. No satisfactory single binding model could be fitted, underscoring the impact of reduced preorganisation. Nevertheless, although less rigid and therefore less discriminating, the acyclic squaratide dimers retain binding ability and provide a platform that, with appropriate modification, may yield useful conformationally adaptable receptor systems.

In summary, we report squaratides, a new peptidomimetic platform that incorporates squaramide hydrogen-bond donors into a peptide-inspired backbone. Side-chain functionality governs self-assembly and anion binding behaviour, tuning affinity, stoichiometry and selectivity, with preference observed for AcO^- and strong Cl^- binding across the series. The modularity of this scaffold makes it a promising platform for potential bioinspired therapeutic peptidomimetics and synthetic anion transport systems.

R. B. P. E., D. T., and K. A. J. conceived and designed the study. F. A. M., C. S. H, S. B., D. T., K.A. J. and R. B. P. E. wrote the manuscript. R. B. P. E. and D. T. supervised the study. F. A. M. and H. T. synthesised the compounds under study and carried out all spectroscopic titrations. C. S. H. carried out X-ray crystallographic analysis. S. B. and D. T. carried out computational analysis. All authors discussed the results and commented on the manuscript.

Conflicts of interest

There are no conflicts to declare.

Data availability

All relevant experimental details, characterisation data, computational data and binding titration data are presented in the main text and supplementary information (SI). Supplementary information is available. See DOI: https://doi.org/10.1039/d6cc00836d.

CCDC 2287336 contains the supplementary crystallographic data for this paper.[30]

Acknowledgements

R. E. and D. T. acknowledge support from Research Ireland (RI) under award number 12/RC/2275_P2 (SSPC) which is co-funded under the European Regional Development Fund. F. M. acknowledges the award of a Hume Scholarship from Maynooth University. R. E. also acknowledges funding from RI for the funding of the NMR facility (12/RI/2346/SOF) through the Research Infrastructure Programme and the Advion Compact Mass Spec through the Opportunistic Infrastructure Fund (16/RI/3399). D. T. and S. B. acknowledge supercomputing resources at the RI/Higher Education Authority Irish Centre for High-End Computing (ICHEC).

References

1 N. Busschaert, C. Caltagirone, W. Van Rossom and P. A. Gale, *Chem. Rev.*, 2015, **115**, 8038–8155.
2 L. K. Macreadie, A. M. Gilchrist, D. A. McNaughton, W. G. Ryder, M. Fares and P. A. Gale, *Chemistry*, 2022, **8**, 46–118.
3 P. A. Gale, E. N. W. Howe and X. Wu, *Chemistry*, 2016, **1**, 351–422.
4 F. A. Mohammed, T. Xiao, L. Wang and R. B. P. Elmes, *Chem. Commun.*, 2024, **60**, 11812–11836.
5 Y. Chen, S. Guerin, H. Yuan, J. O'Donnell, B. Xue, P.-A. Cazade, E. U. Haq, L. J. W. Shimon, S. Rencus-Lazar, S. A. M. Tofail, Y. Cao, D. Thompson, R. Yang and E. Gazit, *J. Am. Chem. Soc.*, 2022, **144**, 3468–3476.
6 L. Chen, S. N. Berry, X. Wu, E. N. W. Howe and P. A. Gale, *Chemistry*, 2020, **6**, 61–141.

7 R. B. P. Elmes and K. A. Jolliffe, *Chem. Commun.*, 2015, **51**, 4951–4968.
8 G. E. Sergeant and K. A. Jolliffe, *Supramol. Chem.*, 2020, **32**, 233–237.
9 J. Bartl and S. Kubik, *ChemPlusChem*, 2020, **85**, 963–969.
10 R. B. P. Elmes, K. K. Y. Yuen and K. A. Jolliffe, *Chem. – Eur. J.*, 2014, **20**, 7373–7380.
11 P. G. Young and K. A. Jolliffe, *Org. Biomol. Chem.*, 2012, **10**, 2664–2672.
12 S. Kubik, *Molecules*, 2022, **27**, 2821.
13 S. Kubik, C. Reyheller and S. Stüwe, *J. Inclusion Phenom. Macrocyclic Chem.*, 2005, **52**, 137–187.
14 S. Kubik, *Chem. Soc. Rev.*, 2009, **38**, 585–605.
15 J. W. Meisel, C. T. Hu and A. D. Hamilton, *Org. Lett.*, 2019, **21**, 7763–7767.
16 N. Rodríguez-Vázquez, M. Amorín, I. Alfonso and J. R. Granja, *Angew. Chem., Int. Ed.*, 2016, **55**, 4504–4508.
17 A. Fuertes, M. Amorín and J. R. Granja, *Chem. Commun.*, 2020, **56**, 46–49.
18 S. S. Burade, S. V. Pawar, T. Saha, N. Kumbhar, A. S. Kotmale, M. Ahmad, P. Talukdar and D. D. Dhavale, *Beilstein J. Org. Chem.*, 2019, **15**, 2419–2427.
19 V. Diemer, L. Fischer, B. Kauffmann and G. Guichard, *Chem. – Eur. J.*, 2016, **22**, 15684–15692.
20 L. Martínez-Crespo, E. C. Escudero-Adán, A. Costa and C. Rotger, *Chem. – Eur. J.*, 2018, **24**, 17802–17813.
21 H. Tong, F. Ali Mohammed and R. B. P. Elmes, *Results Chem.*, 2024, **11**, 101777.
22 L. K. Kumawat, C. Wynne, E. Cappello, P. Fisher, L. E. Brennan, A. Strofaldi, J. J. McManus, C. S. Hawes, K. A. Jolliffe, T. Gunnlaugsson and R. B. P. Elmes, *ChemPlusChem*, 2021, **86**, 1058–1068.
23 R. B. Elmes, P. Turner and K. A. Jolliffe, *Org. Lett.*, 2013, **15**, 5638–5641.
24 L. Qin, A. Hartley, P. Turner, R. B. P. Elmes and K. A. Jolliffe, *Chem. Sci.*, 2016, **7**, 4563–4572.
25 D. Brynn Hibbert and P. Thordarson, *Chem. Commun.*, 2016, **52**, 12792–12805.
26 N. Busschaert, I. L. Kirby, S. Young, S. J. Coles, P. N. Horton, M. E. Light and P. A. Gale, *Angew. Chem., Int. Ed.*, 2012, **51**, 4426–4430.
27 D. O. Soloviev and C. A. Hunter, *Chem. Sci.*, 2024, **15**, 15299–15310.
28 C. Acconcia, A. Paladino, M. D. Valle, B. Farina, A. Del Gatto, S. D. Gaetano, D. Capasso, M. T. Gentile, G. Malgieri, C. Isernia, M. Saviano, R. Fattorusso, L. Zaccaro and L. Russo, *Int. J. Mol. Sci.*, 2022, **23**, 11039.
29 J. Damjanovic, J. Miao, H. Huang and Y. S. Lin, *Chem. Rev.*, 2021, **121**, 2292–2324.
30 CCDC 2287336: Experimental Crystal Structure Determination, 2026, DOI: 10.5517/ccdc.csd.cc2gs51h.